Segmental Dynamics and Density Fluctuations in Polymer Networks during Chemical Vitrification

Benjamin D. Fitz and Jovan Mijovic*

Department of Chemical Engineering and Chemistry, Polytechnic University, Brooklyn, New York 11201

Received September 11, 1998; Revised Manuscript Received March 26, 1999

ABSTRACT: Molecular dynamics of network-forming reactive polymers were examined as a function of the advancement of chemical reaction as the materials structure undergoes a transition from liquid to amorphous solid. The accompanying changes in the segmental relaxation time (α process) are a signature of the materials state (within the liquid to amorphous solid spectrum of physical properties). Both broadband dielectric relaxation spectroscopy (DRS), which probes the α process via dipolar reorientational mobility, and dynamic light scattering (DLS), which probes the α process via density fluctuations, were used to monitor the system under reaction conditions in the reaction bath (to our knowledge, the first study of its kind). An excellent agreement was found between DRS and DLS for the α process characteristic parameters: relaxation time and KWW, the stretched exponential parameter (characterizing the relaxation breadth). That dipole dynamics exhibit the same α relaxation characteristics as time dependent density fluctuations, suggests that the rotational motion observed in a DRS measurement is directly controlled by the behavior of the density domains. It was concluded that the broadening of the α process is due to a general phenomenon: the micro/nanoscale heterogeneous nature of glass formers. The results of the study are discussed in terms of cooperative and local relaxation modes in the growing network.

I. Introduction

The glass transition is an intriguing phenomenon—it has been widely studied, it is encountered in nearly every material processing situation, and yet the underlying physics are not completely understood.[1] It is customary to investigate the problem by studying the temperature dependence of some material response (relaxation) to an applied perturbation in a chemically stable material. The glass transition is then defined as the temperature range where the relaxation time is on the order of 10^2 seconds. It is also possible to observe the formation of a glass via a chemical reaction in network-forming polymers: miscible liquid reactants with a glass transition temperature (T_g) much lower than the reaction temperature react to form a network with a T_g that exceeds the reaction temperature. The material relaxation time will increase during the reaction from liquidlike values (picoseconds) to glassy values (10^2 s) at the completion of the reaction. Of interest in this work is to examine the effect of advancement of reactions on network dynamics as described by segmental motions and density fluctuations.

The material relaxation process associated with T_g is conventionally named the α relaxation and is associated with cooperative segmental molecular motions and with microscale fluctuations of density. The α process is to be distinguished from other modes of material response such as diffusion-related, molecular translational processes, and from local, submolecular, secondary processes. Secondary processes generally fall into the discussion of T_g-related relaxations and have the following characteristics: located at high frequencies (short time scales $<10^{-5}$ s), broad dispersions, Arrhenius temperature dependence, low activation energy ~5 kcal/mol K, low intensity, and are present above and below T_g. The origin of these so-called β relaxations remains elusive, but appeals have been made in the literature to explanations ranging from far-IR phonon excitations,[2] cage-rattling motions,[3,4] a universal glassy-state phenomena,[5] and various types of local/side-chain motions.[6,7] For the purpose of this article we rest with providing an operational definition of the process. At high temperatures (and therefore frequencies) the α and β processes merge; the faster-moving (with temperature) α process catches up with and merges with the slower moving (with temperature) β process to become the $\alpha\beta$ process.

The relaxation time and spectral shape of the α process may be quantified via the stretched exponential relaxation function KWW

$$\phi(t) = Ce^{-(t/\tau)^{\beta}} \tag{1}$$

credited to Kohlrauch, Willams, and Watts,[8] where C is a constant, τ is the relaxation time, and β is the stretching exponent ranging from 0 to 1. For a chemically stable material on cooling from the liquid the relaxation function tends to broaden (the β parameter decreases) as T_g is approached,[9,10,11] this phenomena is explained by both an increase in intermolecular cooperativity[12] and the increased influence of high-frequency secondary relaxation events.[13,14] Unfortunately, a complete understanding of the relaxation function broadening due to temperature is complicated by the fact that relaxation phenomena near T_g are generally nonlinear events and as such contain a time and thermal history dependent relaxation time.[15−17] Nonlinearity is explained by the fact that when decreasing the temperature near T_g and below, the increase in the materials density becomes kinetically hindered—the time lag from a given temperature down-jump to the new equillibrated density is termed structural relaxation (or physical aging), eventually at sufficiently low temperatures the kinetics for reestablishment of structural equillibrium become prohibitively slow. The nonlinearity also makes

* To whom correspondence should be addressed.

10.1021/ma981435y CCC: $18.00 © 1999 American Chemical Society
Published on Web 05/26/1999

necessary the duration of measurement in this temperature range to be very short compared with the process being measured—there are no experimental techniques presently available to adequately fulfill this requirement.

α and β processes have been investigated by numerous techniques. Spectroscopic techniques include NMR,[18,19] neutron diffraction,[20,21] dielectric relaxation spectroscopy (DRS),[22] dynamic light scattering (DLS),[23] and X-ray photon correlation spectroscopy.[24] There are also the conventional techniques which rely on a mechanical perturbation: viscoelastic techniques,[15] acoustic and ultrasonic methods,[25,26] and the calorimetric approaches.[27,28,29] The DRS and DLS techniques stand out among these for their wide-frequency capabilities, rapid measurement times, and high sensitivity. These features lend themselves to the study of the evolution of α and β processes in chemically reactive systems. To our knowledge a study of the development of these processes has not been reported for a chemically reactive network-forming thermoset system using DLS and no comparison has been made between DRS and DLS on these systems. An important question is whether the time scales of segmental motions and density fluctuations during network formation evolve at commensurate or disparate rates. To address this question we first briefly discuss the material properties yielded by DRS and DLS that are relevant to describing network dynamics.

II. Theoretical and Experimental Background

Dielectric Relaxation Spectroscopy. The material response to the **E** field is via several polarization mechanisms: (1) high-frequency induced polarizations: atomic-electronic (in this frequency range the measured dielectric constant is equal to the square of the index of refraction of the material), (2) polarization of permanent dipoles, that is, dipolar rotation/reorientation/translation, and (3) polarizations via conduction processes, that is, translation of charge carriers and nontranslational charge-transfer mechanisms (e.g., hydrogen bonding). For the purposes of this paper, we focus on regime 2, where the motion of dipoles dominates. The polarization decay in this regime, in terms of complex permittivity may be written as

$$\frac{\epsilon^*(i\omega) - \epsilon_\infty}{\epsilon_0 - \epsilon_\infty} = 1 - i\omega\int_0^\infty [\exp(-i\omega t)]\phi(t)\mathrm{d}t \qquad (2)$$

where ϵ_0 is the low-frequency maximum value of the dielectric constant, ϵ_∞ is the high-frequency dielectric constant, ω is angular frequency, and $\phi(t)$ is the relaxation kernel, often modeled by eq 1. $\phi(t)$ may also be obtained from the dipole correlation function

$$\phi(t) = \frac{\sum_i^N \sum_j^N \langle \mu_i(0)\mu_i(t)\rangle}{\sum_i^N \sum_j^N \langle \mu_i(0)\mu_i(0)\rangle} \qquad (3)$$

where $\mu_i(t)$ denotes the elementary dipole moment on the molecule at time t.[30] It is sufficient to use only one portion of the real or imaginary complex permittivity, since they are related by the Kramers−Kronig transform, then by taking the imaginary part of the Fourier transform of eq 2 we obtain:

$$\phi(t) = \frac{2}{\pi}\int_0^\infty \frac{\epsilon''(\omega)}{\epsilon_0 - \epsilon_\infty}\frac{\cos(\omega t)}{\omega}\mathrm{d}\omega \qquad (4)$$

However, instead of transforming the frequency domain dielectric data into the time domain using a discrete Fourier transform, where spectral features may be truncated, we instead transform the relaxation kernel (eq 1) into the frequency domain by using the technique described by Dishon et al.[31] and then fit the experimental data to the transformed kernel with appropriate parameters.

The measured complex permittivity thus contains information which is unique to the molecular-level composition of the material. The interpretation of the polarization response, because the energy changes involved in the various polarization mechanisms are widely distributed and the values of $h\omega/kT$ are low, does not require a quantum mechanical treatment and can proceed from classical electromagnetic theory.[32,33]

Dynamic Light Scattering (DLS). DLS enables the measurement of the intensity autocorrelation function, $g_2(\bar{q},t)$, defined as

$$g_2(\bar{q},t) = \frac{\langle I(\bar{q},0)I(\bar{q},t)\rangle}{\langle I\rangle^2} \qquad (5)$$

where I is the time dependent light scattering intensity, $\langle\ \rangle$ represents the long time average, and $\bar{q}$ is the scattering vector,

$$\bar{q} = \frac{4\pi n}{\lambda_0}\sin\left(\frac{\theta}{2}\right) \qquad (6)$$

where n is the index of refraction of the medium, λ_0 is the vacuum beam wavelength, and θ is the scattering angle, and these parameters are related to the normalized electric field autocorrelation function $g_1(\bar{q},t)$ assuming the conditions are satisfied (given a particular experimental situation) for the validity of the Siegert relation, in the following way:

$$g_1(\bar{q},t) = (g_2(\bar{q},t) - 1)^{1/2}\left(\frac{1}{f}\right)^{1/2} \qquad (7)$$

where f is a constant depending on the experimental setup. The measured g_2 data may be treated as a relaxation function and fitted to eq 1 or, alternatively, the spectral distribution of the scattered light may be obtained from

$$S(\bar{q},\omega) = \frac{1}{2\pi}\int_{-\infty}^{\infty}\exp(-i\omega t)g_2(\bar{q},t)\mathrm{d}t \qquad (8)$$

Controlling the scattering vector $\bar{q}$ allows for the probing of a particular length-scale in a material, $l = 2\pi/|\bar{q}|$. Experiments using conventional laser light sources are capable of probing the limit of $|\bar{q}|$ approaching $0-\sim 10^{-3}$ Å^{-1}. It has been found that the time dependent scattering from density fluctuations is independent of $\bar{q}$ in this range;[34,35,36] however, when the length-scale approaches the scale of cooperative molecular rearrangements which give rise to the α process, a $\bar{q}$ dependence should arise. This work has not been attempted because of the experimental difficulties involved in working in the intermediate $\bar{q}$ range: the DLS

technique is not capable of measuring a large enough $\bar{q}$, while the smallest $\bar{q}$ presently available in quasi-elastic neutron scattering is too large.[37,38] Nevertheless, preliminary studies have been undertaken by Arbe et al.[39] who have found a $\bar{q}$ dependence for the α process in the range of 0.3 to 3 $Å^{-1}$. Other attempts to determine the length scale are the following. Recent dielectric experiments on materials confined to a range of nanometer-scale porous glasses where the α process length scale was determined to be ∼2 nm.[40,41] Also work on a homologous oligomer-to-polymer series where a crossover for the dynamics of the α process from a molecular weight dependent regime to a molecular weight independent regime. A critical chain length of 25 backbone atoms was found in that work and from which a ∼2−3 nm length-scale for the α process was inferred.[42] In any case, the present work is not concerned with the $\bar{q}$ dependence of the α process, and although the index of refraction of the material under study changes during the chemical reaction, the resulting $\bar{q}$ change (see eq 6) will not influence the measured α process parameters (KWW τ and β, eq 1).

The principal objective of this study is to explore the process of glass formation via a chemical reaction in network-forming polymers. To this end, measurements by DRS and DLS were employed to observe the reaction-induced changes in dipolar and density fluctuation relaxation characteristics. The results of the study are presented and discussed in terms of cooperative and local relaxation modes.

III. Experimental Section

Materials. The material requirements were outlined previously: a material which is initially a liquid which gradually reacts to form a glassy solid. We have used a two component reactive mixture: DGEBA (diglycidyl ether of bisphenol A), molecular weight of 374 g/mol (Aldrich, used as-received), and DETA (diethylenetriamine) (Acros, used as-received). The structures are given below

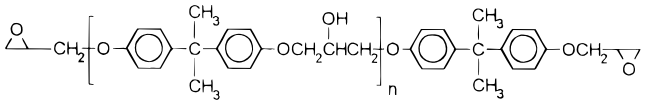

DGEBA (diglycidylether of Bisphenol-A), n<0.1

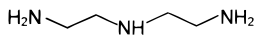

DETA (diethylenetriamine)

The liquids were mixed in the stoichiometric molar ratio DGEBA:DETA of 5:2 for 2 min and immediately transferred to the appropriate measurement cells and tested. The reaction chemistry is via the well-known step-growth polymerization.[43] The step-growth nature of the reaction ensures that the changes in the material are homogeneous and that the molecular weight distribution changes in a systematic fashion. For the low temperature frequency sweeps, the samples were quenched to the lowest measurement temperature, allowed to thermally equillibrate and then swept. All subsequent measurement temperatures were arrived at by heating at 2 °C/min, followed by a hold until thermal equillibrium was gained. No significant chemical reaction occurs during these frequency sweeps.

The chemical changes during isothermal heating of the reactive mixture were monitored by near-infrared spectroscopy (NIR); the details of our use of the technique may be found elsewhere.[44] The NIR spectra are presented in Figure 1 which indicate the disappearance of epoxide and amine groups and the formation of hydroxyl groups. The relative concentration

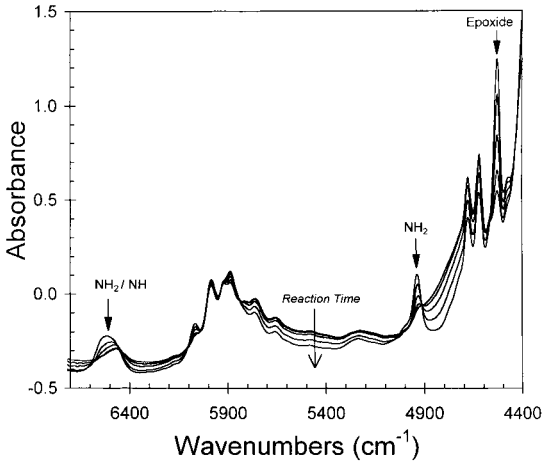

Figure 1. NIR spectra during isothermal cure of DGEBA/DETA at 50 °C at different extents of epoxide conversion. Functional group assignments of several bands are indicated.

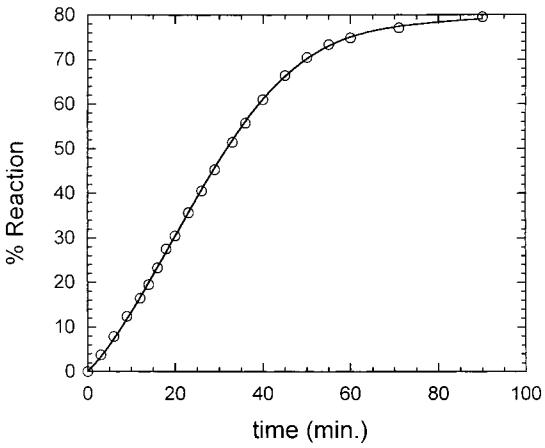

Figure 2. Extent of cure as a function of reaction time.

of epoxide groups is determined by comparison of the area under the epoxide peak at a given reaction time to the initial peak area, and normalizing using a group peak which is not involved in the reaction (in this case the aromatic C−H stretch at 4673 cm^{-1}):

$$\% \text{ group conversion} = 100\%*\left[1 - \frac{A_{ref}(0)*A_{group}(t)}{A_{ref}(t)*A_{group}(0)}\right] \quad (9)$$

The extent of reaction of epoxide groups as a function of reaction time is presented in Figure 2.

The maximum T_g attainable for the fully reacted mixture is 129 °C as determined by DSC (10 °C/min, 10 mg. sample). The extent of reaction at which the system forms a gel from the classical Flory calculation is ∼50%.[43]

Dynamic Light Scattering. A comprehensive description of the light-scattering apparatus used may be found elsewhere.[45] The reactants were prepared in the same manner as for the dielectric experiments. The homogeneous reactive mixture was then added to a dust-free test tube of diameter 10 mm. The sample was placed in the light scattering sample holder in a toluene bath maintained at 50 °C. The light source was a diode-pumped solid-state laser operating at wavelength of 530 nm, with a power of 100mW. The measurement was performed in the unpolarized homodyne mode. The full correlation functions were obtained using an ALV5000 autocorrelator. The measurement time of a single correlelogram was set to 1 min to ensure that no significant chemical reaction takes place during the measurement.

Dielectric Relaxation Spectroscopy. A detailed description of our experimental facility for dielectric measurements is given elsewhere.[46] However, briefly, we have used an

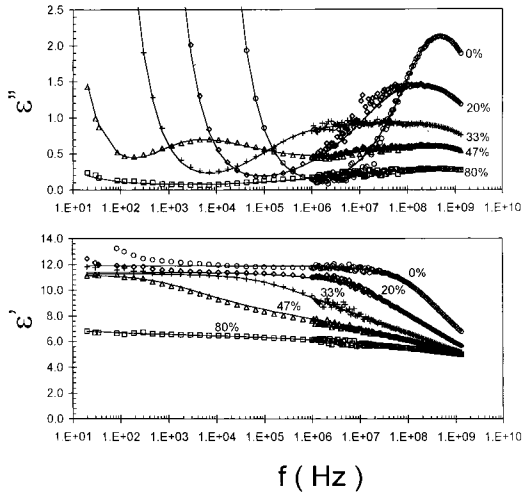

Figure 3. Dielectric constant and loss in the frequency domain at different extents of cure forDGEBA/DETA isothermal reaction at 50 °C. The solid line is a fit to a two term Havrilliak−Negami function.

HP4284A impedance analyzer to cover the frequency range: 20 Hz to 1 MHz; from 1 to 1600 MHz an HP4291A impedance analyzer was used in conjunction with a sample cell, high precision extension air line, and calibration software from NOVOCONTROL GmBh; and an HP8752A network analyzer was also used for the range 10 (MHz−1.3 GHz, making use of our own modified sample cell and software to calculate the complex dielectric constant from the measured reflection coefficients.

IV. Results and Discussion

We first present the dielectric experimental data. Frequency sweeps of dielectric constant and loss are shown in Figure 3. These data were collected during the reaction under reaction conditions, and the data collection times were correlated with the degree of cure obtained by FTIR. At 0% reaction there is only one relaxation peak (the $\alpha\beta$ process) at 530 MHz with a significant migrating charge contribution at lower frequencies. With increasing conversion the relaxation peak broadens, its intensity diminishes and at 33% the separation of a low-frequency component (α relaxation) is evident. The α process moves to lower frequencies with increased conversion while the high frequency β peak remains. The separation and evolution of the α relaxation toward the glass transition (we are referring to the conventional operational definition of T_g as the temperature where the relaxation time is on the order of 100 s) is clearly illustrated in Figure 4 where we plot the $\alpha\beta$, α, and β relaxation times [τ is the reciprocal of the frequency (as radians/s) at the ϵ'' maximum] as a function of conversion. Examination of the molecular moieties that give rise to the α and β processes has been made in our previous work.[46]

Now, let us give an interpretation of the microscopic events underlying the above results. The separation of the α and β processes is an indication of the increasing number of molecular segments required to cooperate (increasing average domain size) in order for the α relaxation to occur. At any instant, there is a distribution of such domains. These are the regions of differing density underlying the density fluctuations observed via DLS (see later in this section). The unreacted mixture response ($\alpha\beta$ process) is essentially of a local nature due to a large degree of thermal kinetic energy; all motions are within domains of similar size and the number of

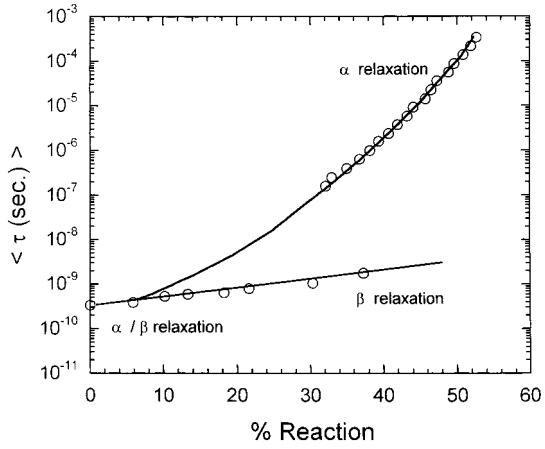

Figure 4. Apparent relaxation time extracted from data of Figure 3 vs extent of cure. Solid lines are guides for the eye.

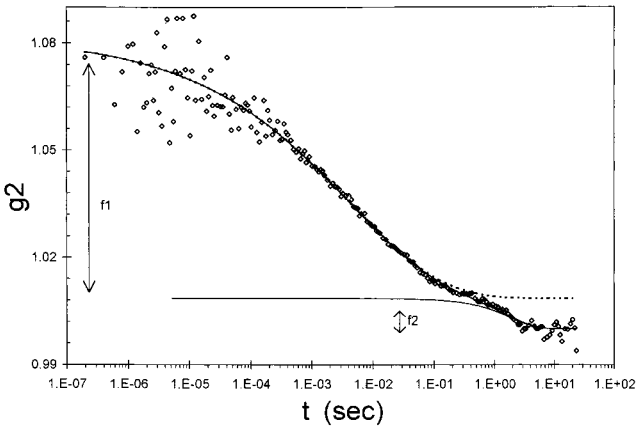

Figure 5. Example of dynamic light scattering intensity correlation function collected during isothermal cure (55% conversion). The solid lines are the individual terms and the composite sum of the KWW model, eq 10.

atoms involved in the relaxation (number of atoms per domain) is small. As the reaction progresses the increasing molecular connectivity leads to a wider distribution of domain sizes (a measure of the broadening distribution is the decreasing KWW β parameter) and of the largest domains, an increase in the number of atoms per domain. When the domain size is much larger than the scale of local motions we observe the splitting into distinct α and β processes, beyond this time in the reaction the α process continues to evolve to longer relaxation times.

The DLS data are examined next. Since the faster β process is unobservable with our experimental DLS facilities, we present the DLS results only for the evolution of the α process during network formation. We emphasize here that in the conversion range to be discussed in the following, the DLS correlation functions are measuring the α process density fluctuations, distinct from concentration, cluster, or optical anisotropy fluctuations. A investigation focused on the identification and distinction between these processes has been reported by Gerharz et al.[34] An example of the dynamic light, scattering intensity correlation function collected during isothermal cure (55% conversion) is shown in Figure 5. The solid lines are the individual terms and the composite sum of the KWW model, eq 10. Our measurements of the experimental intensity correlation raw data at selected conversions between 46% and 72% reaction are presented in Figure 6, where the symbols

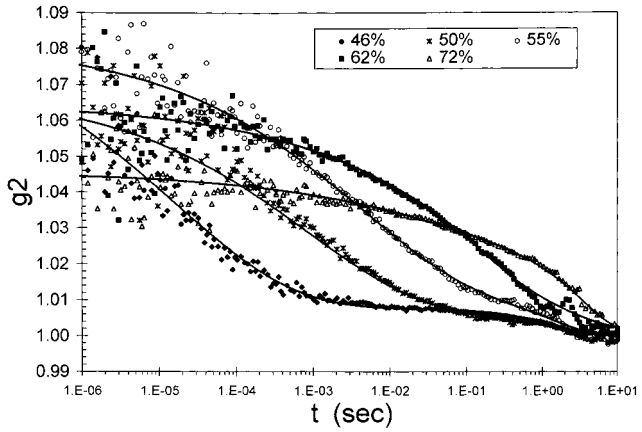

Figure 6. Dynamic light scattering intensity correlation functions collected during isothermal cure. Symbols are raw data; solid lines are best-fit KWW curves.

Table 1. Extent of Reaction Dependence of the Fit Parameters *C*, τ, $\langle\tau\rangle$, β from the KWW Equation [Eq 10] for the α Process from DLS Measurement

	α process				long-time process		
%rxn	$f1$	τ	$\langle\tau\rangle$	β	$f2$	τ	β
39	0.099	5.0×10^{-7}	1.4×10^{-6}	0.28	0.0089	0.1	1
45	0.055	4.0×10^{-5}	3.8×10^{-5}	0.28	0.0075	1.0	1
50	0.060	7.0×10^{-5}	1.0×10^{-4}	0.28	0.0060	2.0	1
56	0.060	5.0×10^{-4}	9.5×10^{-4}	0.28	0.0050	2.0	1
59	0.060	9.6×10^{-4}	1.2×10^{-2}	0.28	0.006	2.0	1
63	0.070	9.0×10^{-2}	7.4×10^{-2}	0.28	0.006	2.0	1
66	0.059	6.8×10^{-2}	1.5×10^{-1}	0.28	0.006	2.0	1
69	0.052	8.0×10^{-1}	2.9×10^{-0}	0.28	0.001	7.0	1
72	0.044	1.6×10^{0}	5.8×10^{0}	0.28	0		

are experimental data and the solid lines represent a best-fit sum of two KWW functions:

$$g2(t) = f_1 \exp[-(t/\tau_1)^{\beta 1}] + f_2 \exp[-(t/\tau_2)^{\beta 2}] + 1 \qquad (10)$$

where the meaning of the variables is the same as eq 1. We note that this model of the data is acceptable; since $f_2 \ll f_1$, the respective τ's are sufficiently separated, and the β_2 parameter has been fixed at a constant value of 1. The KWW parameters are given in Table 1. It should be noted that for all degrees of conversion from 36% to 72% the KWW β parameter for the α process is 0.28 ± 0.02, indicating a wide breadth for the process over this range of conversion. It should also be noted that the KWW apparent relaxation times are in agreement with those obtained by the distribution-fitting CONTIN[47] routine. The minor, second KWW term (at long times) we consider to be independent of the α process. This approach has been reported previously by Tabellout et al.,[48] and for the purposes of this paper we do not consider it further. Speculations have been made on the origin of long-term relaxations in a similar proximity to the α process by Fisher et al.,[49,50] who studied small molecules and polymers and postulated the existence of clusters as a general feature of the amorphous state; however, the statistical error in our data at long times does not permit a definitive conclusion on this issue.

To compare the dielectric and light-scattering spectra we employ the same KWW relaxation function Fourier transformed into the frequency domain in Figure 7 (A–C). We show in plot A KWW fits to a master curve of the 0% data shown at several temperatures and the same in plot B for a 10% conversion sample. The KWW β parameter is 0.40 for both conversions. The KWW fit

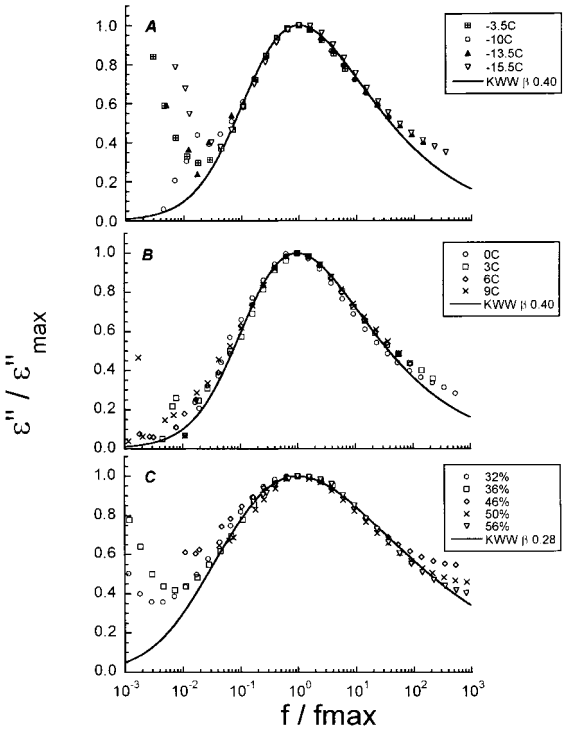

Figure 7. Normalized dielectric loss for DGEBA/DETA at various extents of cure: (A) unreacted mixture, at the temperatures indicated; (B) system at 10% reaction, at the temperatures indicated; (C) for indicated extent of reaction at 50 °C *during cure.*

results for the 0% material at 50 °C (not shown in Figure 7) yield a KWW β of 0.45: it is apparent that the distribution of relaxation times broadens with decreasing temperature. The neat DGEBA resin has been found to have a temperature independent β parameter of 0.56,[46] indicating a significantly narrower distribution of relaxation times than the reactive mixture, which leads to the assumption of increased microheterogeneity for the mixture (broadening by concentration fluctuations). In plot C we present isothermal in situ normalized dielectric loss plots, where for a conversion range from 32% to 56% a KWW β parameter of 0.28 represents the best fit, indicating that the distribution of domains does not appreciably change in this conversion range. The KWW β parameters at comparable degrees of cross-linking are in agreement with those found in the literature for similar systems, such as DGEBA/MDA (an aromatic amine) after 60% conversion β is 0.28, while a β of 0.31 was found for a polyurethane gel at full conversion.[48]

We now compare the changes in the α relaxation time, τ, with conversion for the dielectric and light-scattering data together in Figure 8. We obtain τ_{DRS}, as stated above, from the reciprocal of the ϵ'' peak frequencies. For the DLS data, we use the following well-known relation to connect the apparent relaxation time to the KWW τ

$$\langle\tau_{app}\rangle = \tau^*\Gamma\left(\frac{1}{\beta}\right) \qquad (11)$$

where Γ is the Gamma function. As seen in Figure 8 the agreement in relaxation times between the two techniques is very good.

It seems reasonable to conclude that since the DLS and DRS results are in agreement, the underlying origin

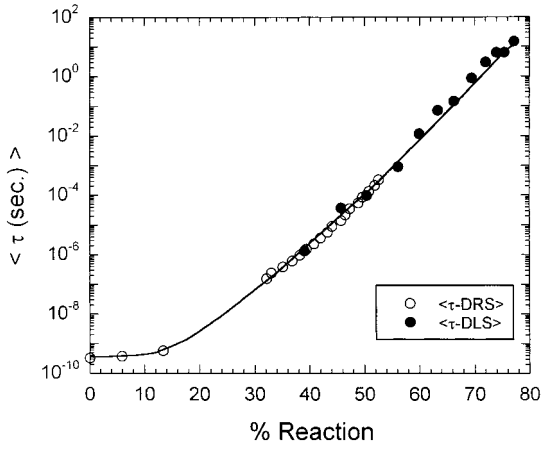

Figure 8. Apparent relaxation time from DLS and DRS experiments vs extent of cure forDGEBA/DETA at 50 °C. Solid lines are guides for the eye.

of the α process is the same. We will discuss shortly the implications. We first mention the conflicting evidence found in the literature for other comparisons between DRS and DLS data. For some polymers: PPG, PVAc, PS, and PEA it was found that when comparing data at the same temperature $\tau_{DRS} < \tau_{DLS}$ and the KWW parameter $\beta_{DLS} < \beta_{DRS}$.[51] While for other polymers, including PMPS,[52] PHMA,[53] and poly(*n*-laurel methacrylate)[54] and for low molecular weight liquids BKDE and BCDE,[55] the α processes have equivalent τ and KWW β parameters.

The next point of discussion is whether the DLS and DRS measurements on the α process are sensitive to gel formation. Studies of gels and gel-formation via DLS (for example, refs 56−58) are generally concerned with concentration fluctuations. These studies are performed at temperatures much higher than the glass transition temperature where the α process is in the picosecond range, well beyond the short time window of conventional autocorrelators. In this work, we focus on the conversion range where the α process enters the correlator window from the short time side and crosses through to the long time region with the advancement of cross-linking reactions. In the sol−gel regime of the previous studies on gelation,[56−58] critical behavior near the gel point is manifest as a sudden change in the intensity correlation function from a stretched exponential to a power law, analogous to similar behavior observed via viscoelastic measurements.[59] We do not expect to find such a crossover since we are making observations on a fundamentally different relaxation process. This prediction is confirmed since for both DLS and DRS there do not appear to be any remarkable changes in the relaxation characteristics on crossing the gel point. The KWW relaxation form is retained and the β parameter is also unchanged, while the relaxation time increases in a continuous manner. The fact that measurements on the α process are not sensitive to gelation stems from the length-scale of the process, as stated in the Introduction the current consensus for this scale is on the order of 1−5 nm. Experiments probing such a small scale could not, in general, be revealing for a macroscopic event such as gelation.

V. Conclusions

The α relaxation on a glass-forming reactive system has been monitored using both DLS and DRS techniques during network and glass formation. The KWW stretched exponential relaxation functional form has been applied to measurements from both techniques in order to quantitatively compare them. The relaxation characteristics are in excellent agreement between the two techniques. The KWW relaxation function implies either a distribution of simple exponential processes or a single process inherently slowed beyond the exponential decay. The former explanation is in accord with the following reasoning. In the conversion range where the α process has an associated time-scale slow enough to be found within the DLS autocorrelation time window, the DLS experiment is measuring longitudinal density fluctuations (at lower conversions we measure a different process, concentration fluctuations, not discussed in the text). The connection between the micro-Brownian α process, the glass transition, and density fluctuations observed via DLS has been amply demonstrated in the literature. At any given instant, the fluctuating density will be frozen, and a hypothetical instantaneous microscopic snapshot is that of a distribution of domains of various densities (the macroscopic density being the ensemble average of these subsystems). Regions of higher density are assumed to relax more slowly, lower density more quickly; the distribution of density domains thus yields the distribution of relaxation times. That dipole dynamics exhibit the same α relaxation characteristics as time dependent density fluctuations suggests that the α process as measured by DRS is also broadened by the density domain heterogeneity. The factors influencing the density domains are evidently also those that govern both the distribution of dipolar relaxation times and the mean of the relaxation times for the α process.

On the temperature dependence of domains, we may speculate that the size of the domains decreases with increasing temperature, which would be in agreement with the thermodynamic arguments of Adam and Gibbs.[60] We know that the time scale of the fluctuations also decreases with increasing temperature, so that there is an increased averaging effect due to the rapid interconversion of domains at high temperatures. These interconversions decrease at temperatures close to T_g (in this case, instead of temperature as a variable, with increasing cure), this may explain the distribution of relaxation times increasing with cure.

At present a molecular theory for the description of the domain sizes and dynamics is lacking. Such a theory would have to account for the distribution of domain sizes and the temperature dependence of the distribution and be based on specific chemical features of the material.

Finally, we have demonstrated the possibility of monitoring cure via changes in the α relaxation time using DRS and for the first time DLS.

Acknowledgment. This material is based on work supported by the National Science Foundation under Grant DMR-9710480. We thank Amy Lefebvre for conducting the light-scattering experiments.

References and Notes

(1) For selected reviews, see: (a) Ediger, M. D.; Angell, C. A.; Nagel, S. R. *J. Chem. Phys.* **1996**, *100*, 13200. (b) Stillinger, F. H. *Science* **1995**, *267*, 1935. (c) Angell, C. A. *Science* **1995**, *267*, 1924. (c) Jäckle, J. *Rep. Prog. Phys.* **1986**, *49*, 171. For monographs, see: (a) *Structure and Dynamics Of Glasses and Glass Formers*; In *Proceedings of the MRS Symposium*; Angell, C. A., Ngai, K. L., Kieffer, J., Egami, T., Nienhaus,

G., Eds.; MRS Publ.: Pittsburgh, PA, 1997; Vol. 455. (b) *Relaxations in Complex Systems*; Ngai, K. L.; Wright, G., Eds.; National Technical Information Service, U.S. Department of Commerce: Springfield, VA, 1984. (c) Colmenero, J. *Basic Features Of The Glassy State*; World Scientific: Singapore, 1990. (d) *Dynamics of Disordered Materials II*; Dianoux, A. J., Petry, W., Richter, D., Eds.; North-Holland: Amsterdam, 1993. (e) Hansen, J. P., Levesque, D., Zinn-Justin, J., Eds. *Liquids, Freezing and the Glass Transition*; North-Holland: Amsterdam, 1991.

(2) Angell, C. A.; Boehm, L.; Oguni, M.; Smith, D. L. *J. Mol. Liq.* **1993**, *56*, 275.
(3) Johari, G. P. In *Relaxations in Complex Systems*; Ngai, K. L., Wright, G., Eds.; National Technical Information Service, U.S. Department of Commerce: Springfield, VA, 1984.
(4) Lewis, L. J.; Wahnstrom, G. *Phys. Rev. E* **1994**, *50*, 3865.
(5) Johari, G. P.; Goldstein, M. *J. Chem. Phys.* **1970**, *53*, 2372.
(6) McCrum, N. G.; Read, B.; Williams, G. *Anelastic And Dielectric Effects In Polymeric Solids*; Wiley: NY, 1967.
(7) Meier, G.; Fujara, F.; Petry, W. *Macromolecules* **1989**, *22*, 4421.
(8) Williams, G.; Watts, D. C. *Trans. Faraday Soc.* **1970**, *66*, 80.
(9) Floudas, G.; Placke, P.; Stepanek, P.; Brown, W.; Fytas, G.; Ngai, K. L. *Macromolecules* **1995**, *28*, 6799.
(10) Alegria, A.; Goitiandia, L.; Telleria, I.; Colmenero, J *J. NonCryst. Solids* **1991**, *131*−*133*, 457.
(11) Schlosser, E.; Schönhals, A. *Polymer* **1991**, *32*, 2135.
(12) Ngai, K. L.; Rendell, R. W.; Rajagopal, A. K.; Teitler, S. *Ann. N. Y. Acad. Sci.* **1986**, *484*, 150.
(13) Williams, G.; *Trans. Faraday Soc.* **1966**, *62*, 2091.
(14) Du, W. M.; Li., G.; Cummins, H. Z.; Fuchs, M.; Toluse, J.; Knauss, L. A. *Phys. Rev. E.* **1994**, *49*, 2192.
(15) Ferry, J. D. *Viscoelastic Properties Of Polymers*, 2nd ed.; Wiley: New York, 1980.
(16) Scherer, G. *Relaxation in Glasses and Composites*; Wiley: New York, 1986.
(17) Matsuoka, S. *Relaxation Phenomena In Polymers*; Hanser: New York, 1986.
(18) Spiess, H. W. *J. Non-Cryst. Solids* **1991**, *131*−*133*, 766.
(19) Kulik, A. S.; Beckham, H. W.; Schmidt-Rohr, K.; Radloff, D.; Pawelzik, U.; Boeffel, C.; Spiess, H. W. *Macromolecules* **1994**, *27*, 4746.
(20) Richter, D.; Zorn, R.; Farago, B.; Frick, B.; Fetters, *Phys. Rev. Lett.* **1992**, *68*, 71.
(21) Arbe, A.; Richter, D.; Colmenero, J.; Farago, B. *Phys. Rev. E* **1996**, *54*, 3853.
(22) Kremer, F.; Arndt, M. In *Dielectric Spectroscopy of Polymeric Materials*, Runt, J. P., Fitzgerald, J. J., Eds.; American Chemical Society: Washington, DC, 1997.
(23) Fytas, G. *Macromolecules* **1989**, *22*, 211.
(24) Dierker, S. B.; Pindak, R.; Flemming, R. M.; Robinson, I. K.; Berman, L. *Phys. Rev. Lett.* **1995**, *75*, 449.
(25) Onabajo, A.; Dorfmüller, Th.; Fytas, G. *J. Polym. Sci., Polym. Phys. Ed.* **1987**, *27*, 749.
(26) D'arrigo, G.; Paparelli, A.; Bertolini, D.; Cassettari, M.; Salvetti, G.; Tombari, E.; Veronesi, S. *J. Non-Cryst. Solids* **1991**, *131*−*133*, 1991.
(27) Murthy, S. S.; Nayak, S. K. *J. Chem. Phys.* **1993**, *99*, 5362.
(28) Fan, J.; Cooper, E. I.; Angell, C. A. *J. Phys. Chem.* **1994**, *98*, 9345.
(29) Dixon, P.; Nagel, S. *Phys. Rev. Lett.* **1988**, *61*, 341.
(30) Williams, G. *Chem. Rev.* **1972**, *72*, 55.
(31) Dishon, M.; Weiss, G. H.; Bendler, J. T. *J. Res. Nat. Bur. Stand.* **1985**, *90*, 27.
(32) Debye, P. *Polar Molecules*; Dover Publications: New York, 1945.
(33) Fröhlich, H. *Theory of Dielectrics*, 2nd ed.; Oxford University Press: Oxford, 1958.
(34) Gerharz, B.; Meier, G.; Fischer, E. W. *J. Chem. Phys.* **1990**, *12*, 7110.
(35) Meier, G.; Fytas, G. In *Optical Techniques To Characterize Polymer Systems*; Bässler, H., Ed.; Studies In Polymer Science 5; Elsevier: Amsterdam, 1989.
(36) Wang, C. H.; Fytas, G.; Lilge, D.; Dorfmüller, Th. *Macromolecules* **1981**, *14*, 1362.
(37) Frick, B.; Richter, D. *Science* **1995**, *267*, 1939.
(38) Chamberlin, R.; Scheinfein, M. *Ultramicroscopy* **1992**, *47*, 408.
(39) Arbe, A.; Colmenero, J.; Monkenbusch, M.; Richter, D. *Phys. Rev. Lett.* **1998**, *81*, 590.
(40) Floudas, G.; Paraskeva, S.; Hadjichristidis, N.; Fytas, G.; Chu, B.; Semenov, A. *J. Chem. Phys.* **1997**, *107*, 5502.
(41) Arndt, M.; Stannarius, R.; Groothues, H.; Hempel, E.; Kremer, F. *Phys. Rev. Lett.* **1997**, *79*, 2077.
(42) Jacobsson, P.; Borjesson, L.; Torell, L. *J. Non-Cryst. Solids* **1991**, *131*−*133*, 104.
(43) Flory, P. *Principles Of Polymer Chemistry*; Cornell University Press: Ithaca, New York, 1953.
(44) Mijovic, J.; Andjelic, S. *Macromolecules* **1996**, *29*, 239.
(45) Zhao, J. Q.; Pearce, E.; Kwei, T. K.; Jeon, H. S.; Khatri, C.; Balsara, N. *Macromolecules* **1995**, *28*, 1972.
(46) Fitz, B.; Andjelic, S.; Mijovic, J. *Macromolecules* **1997**, *30*, 5227. Andjelic, S.; Fitz, B.; Mijovic, J. *Macromolecules* **1997**, *30*, 5239.
(47) Provencher, S. W. *Comput. Phys. Commun.* **1982**, *27*, 213.
(48) Tabellout, M.; Baillif, P.; Randrianantoandro, H.; Litzinger, F.; Emery, J.; Nicolai, T.; Durand, D. *Phys. Rev. B* **1995**, *51*, 12295.
(49) Fischer, E.; Meier, G.; Rabenau, T.; Patkowski, A. Steffen, W.; Thonnes, W *J. Non-Cryst. Solids* **1991**, *131*−*133*, 134.
(50) Fischer, E. *Phys. A.* **1993**, *201*, 183.
(51) Ngai, K. L.; Mashimo, S.; Fytas, G. *Macromolecules* **1988**, *21*, 3030.
(52) Boese, D.; Momper, B.; Meier, G.; Kremer, F.; Hagenah, J.; Fischer, E. *Macromolecules* **1989**, *22*, 4416.
(53) Hwang, Y.; Patterson, G. D.; Stevens, J. J. *Polym. Sci., Part B Polym. Phys.* **1996**, *34*, 2291.
(54) Floudas, G.; Placke, P.; Stepanke, P.; Brown, W.; Fytas, G.; Ngai, K. L. *Macromolecules* **1995**, *28*, 6799.
(55) Meier, G.; Gerharz, B.; Boese, D.; Fischer, E. *J. Chem. Phys.* **1991**, *94*, 3050.
(56) Rouf-George, C.; Munch, J.; Schosseler, F.; Pouchelon, A.; Beinert, G.; Boue, F.; Bastide, J. *Macromolecules* **1997**, *30*, 8344.
(57) Joosten, J.; McCarthy, J.; Pusey, P. *Macromolecules* **1991**, *24*, 6690.
(58) Martin, J.; Wilcoxon, J.; Odinek, *J. Phys. Rev. A.* **1991**, *43*, 858.
(59) Winter, H.; Morganelli, P.; Chambon, R. *Macromolecules* **1988**, *21*, 532.
(60) Adam, G.; Gibbs, J. *J. Chem. Phys.* **1965**, *43*, 139.

MA981435Y